Journal of Sound and Vibration (1999) **228**(4), 857–870
Article No. jsvi.1999.2451, available online at http://www.idealibrary.com on IDEAL®

IDENTIFICATION FOR CRITICAL FLUTTER LOAD AND BOUNDARY CONDITIONS OF A BEAM USING NEURAL NETWORKS

I. TAKAHASHI

Department of Mechanical Engineering, Kanagawa Institute of Technology,
1030 *Shimo-ogino, Atugi-shi, Kanagawa* 243-0292, *Japan*

(*Received* 28 *July* 1997, *and in final form* 11 *June* 1999)

With the increasing size and complexity of machines and vessels, the inverse problems of continuous bodies are becoming important. In this paper, the possibility of using a Multilayer Perceptron network trained with the Backpropagation Algorithm for detecting the critical flutter load and boundary conditions of tapered beams is studied. The beam model considered is a Timoshenko beam, which, with the use of the transfer matrix method, estimates the changes in various modal parameters caused by the shape parameters and boundary conditions of beams.

1. INTRODUCTION

Light-weight structures have been used extensively in many industrial fields such as in mechanical, aerospace and rocket engineering, and therefore vibration and stability problems of beams have become increasingly important. In particular, the inverse problems of continuous bodies are gaining importance in design practice.

There are a number of papers available on non-conservative instability of beams subjected to follower forces. Bolotin and Leipholz have extensively studied the non-conservative problems of elastic stability, detailed explanations for which are provided in their books [1, 2]. Saito and Otomi [3] have studied the vibration and stability of beams with an attached mass under axial and tangential loads. Irie *et al.* [4] calculated the critical flutter loads of a Timoshenko beam of a cross-section prescribed by an arbitrary function subjected to a follower force of various types. Many researchers [5, 6] have analyzed the non-conservative instability of beams resting on an elastic foundation. De Rosa and Franciosi [7], and Takahashi and Yoshioka [8] have studied the effect of an intermediate support on the stability behaviour of cantilever beams and double beams subjected to follower forces.

The artificial neural network is presently, one of the most rapidly expanding areas of research across many disciplines [9, 11]. In mathematical fields, the neural network is an effective mapping tool–mapping an input vector to an output vector. The application areas are classification, pattern recognition and function

0022-460X/99/490857 + 14 $30.00/0

approximation. The author has used a neural network to detect the damage of the structural element [12].

On the other hand, the identification technique for boundary conditions of continuous bodies is gaining importance, with the increasing size and complexity of machines and vessels. Recently, Yasuda and Goto [13] and Kamiya *et al.* [14] proposed an experimental identification technique for boundary conditions of the beam. Saito *et al.* [15] presented the identification of non-linear support systems by using the transient response. Takahashi [16] proposed an identification method for the axial force and boundary conditions of a beam using neural networks.

In this paper, the possibility of using a multilayer perceptron network trained with the backpropagation algorithm for identifying the critical flutter load and boundary conditions in the structural element is studied. The natural frequencies which are the most fundamental and simplest of the modal parameters are adopted here to estimate the flutter load and boundary conditions. The basic idea is to train a neural network with simulated patterns of the relative changes in natural frequencies and corresponding critical flutter loads and boundary conditions of beams in order to recognize the vibrating behaviour of the beam.

2. APPLICATION TO BEAM STRUCTURE

2.1. ANALYSIS OF BEAM AND DATA AQUISITION

We consider a non-uniform Timeshenko beam of length l, without damping. The origin o is taken at one end of the beam, and the shear center axis is taken as the x-axis. Taking into account the rotatory inertia and shear deformation, the equations of flexural motion of the beam when subjected to a tangential follower force $f^*(x)$, which is distributed over the axis, can be written as [4].

$$\frac{\partial Q^*}{\partial x} - f(x)\frac{\partial^2 w^*}{\partial x^2} + \rho A(x)\omega^2 w^* = 0, \tag{1}$$

$$Q^* - \frac{\partial M^*}{\partial x} + \rho I(x)\omega^2 \psi^* = 0, \tag{2}$$

where ρ is the mass per unit volume, $A(x)$ is the cross-sectional area, and $I(x)$ is the second moment of area of the beam. The variables w^* and ψ^* denote the transverse deflection and the slope due to pure bending respectively. The variable ω is the natural frequency. The bending moment M^* and shear force Q^* respectively are given by

$$M^* = -EI(x)\frac{\partial \psi^*}{\partial x}, \tag{3}$$

$$Q^* = \{\kappa GA(x) + f^*(x)\}\left(\frac{\partial w^*}{\partial x} - \psi^*\right), \tag{4}$$

where E is Young's modulus and G is the shear modulus. The quantity κ is the shearing coefficient [17].

For simplicity of the analysis, the following dimensionless variables are introduced:

$$w^* = wl, \qquad \psi^* = \psi, \qquad Q^* = \frac{EI_0}{l^2}Q, \qquad M^* = \frac{EI_0}{l}M,$$

$$= \frac{x}{l}, \qquad a = \frac{A(x)}{A_0}, \qquad i = \frac{I(x)}{I_0},$$

$$s_0^2 = \frac{A_0 l^2}{I_0}, \qquad p = \frac{l^2}{EI_0}f^*(x). \tag{5}$$

Here A_0 and I_0 are the sectional area and the second moment of area at one end ($x = 0$). The value s_0 is the slenderness ratio at one end. The quantities without an asterisk (*) are the respective dimensionless variables. As a frequency parameter

$$\lambda^4 = \frac{\rho A_0 l^4 \omega^2}{EI_0} \tag{6}$$

is used here.

Equations (1)–(4) for the beam are written as a matrix differential equation

$$\frac{\mathrm{d}}{\mathrm{d}\xi}\{Z(\xi)\} = [U(\xi)]\{Z(\xi)\}, \tag{7}$$

where the state vector $\{Z(\xi)\} = \{w\psi QM\}^{\mathrm{T}}$ and the coefficient matrix $[U(\xi)]$ is

$$U_{11} = 0, \qquad U_{12} = 1, \qquad U_{13} = \frac{1}{g}, \qquad U_{14} = 0,$$

$$U_{21} = 0, \qquad U_{22} = 0, \qquad U_{23} = 0, \qquad U_{24} = -\frac{1}{i},$$

$$U_{31} = \frac{-\lambda^4 a}{(1 - p/g)}, \qquad U_{32} = 0, \qquad U_{33} = \frac{-p}{(1 - p/g)}\frac{g'}{g^2},$$

$$U_{34} = \frac{-p}{(1 - p/g)}\left(\frac{1}{i}\right),$$

$$U_{41} = 0, \qquad U_{42} = i\frac{\lambda^4}{s_0^2}, \qquad U_{43} = 1, \qquad U_{44} = 0,$$

$$\left(\because\ g = \kappa\frac{G}{E}s_0^2 a + p, \quad \frac{G}{E} = \frac{1}{2(1+\nu)}\right), \tag{8}$$

in which the prime denote differentiation with respect to ξ.

Since analytical solutions of equation (7) cannot be obtained for a beam of varying cross-section, the transfer-matrix approach is adopted here. In general, the state $\{Z(\xi)\}$ can be expressed as

$$\{Z(\xi)\} = [T(\xi)]\{Z(0)\} \tag{9}$$

by using the transfer matrix $[T(\xi)]$ of the beam. From equations (7) and (9), the following equation is derived:

$$\frac{\mathrm{d}}{\mathrm{d}\xi}[T(\xi)] = [U(\xi)][T(\xi)]. \tag{10}$$

For a beam of varying cross-section, the matrix $[T(\xi)]$ is obtained by integrating equation (10) numerically with the starting value $[T(0)] = [1]$ (the unit matrix), which is given by taking $\xi = 0$ in equation (9). In the calculation, the elements of the transfer matrix are determined numerically by using the Runge–Kutta integration method.

The method is applied to some beams of varying cross-section, and the eigenvalues of vibration and the critical flutter loads are calculated numerically. Consider a beam whose breadth and depth are expressed as

$$b(x) = b_0 - (b_0 - b_1)\left(\frac{x}{l}\right), \qquad h(x) = h_0 - (h_0 - h_1)\left(\frac{x}{l}\right), \tag{11}$$

where b_0 and b_1 denote the breadth of the two ends, also h_0 and h_1 denote the depth.

Tangential forces of the following types are considered.

A concentrated follower force-Beck's problem: when a concentrated follower force F_B acts at the free end, p is written as

$$p = p_B, \quad (p_B = F_B l^2/EI_0), \tag{12}$$

where p_B denotes the dimensionless force parameter.

The numerical calculations were carried out for the free-elastically restrained beams subjected to a concentrated follower force, as shown in Figure 1. The beam is elastically restrained against rotational motion by springs of the dimensionless stiffness k'. For the cantilever beam, k' is finite. The origin of the axis is taken at elastically restrained end.

The method is applied to beams with linearly varying depth h_1/h_0 and breadth b_1/b_0, and the natural frequencies are calculated numerically, to provide information about the effect on these with varying cross-section, critical flutter load and boundary conditions. In the following section, we will discuss the three effects of the taper ratio, boundary conditions and slenderness ratio on the critical flutter load of the tapered beam subjected to a constant follower force at the free end.

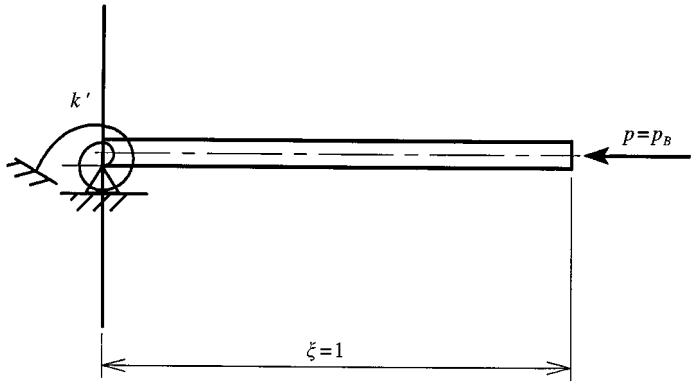

Figure 1. Free-elastically restrained beam.

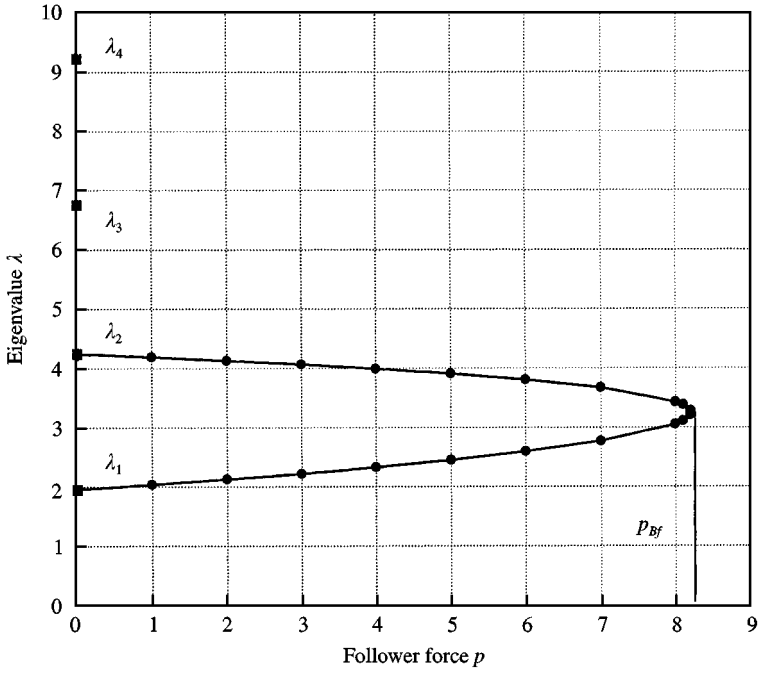

Figure 2. Eigenvalue curve.

Figure 2 shows the eigenvalue curve of a cantilever beam subjected to a concentrated follower force at the free end. The values ($\lambda_1 - \lambda_4$) of the curve on the ordinate indicate the eigenvalues of the beam without the action of the follower force. With increasing force, the eigenvalues of the first mode increase, while those of the second mode decrease. The maxima of the branch of the eigenvalue curve indicates the critical flutter load p_{Bf} beyond which the natural frequencies become complex quantities and therefore, the motion becomes an unstable vibration with exponentially increasing amplitude.

TABLE 1

Critical flutter load of the cantilever beam ($v = 0{\cdot}3$, $b_1/b_0 = 1{\cdot}0$, $s_0 = 50$)

	Timoshenko		Classical	
h_1/h_0	Kounadis and Katsikadelis [18]	Present	Bolotin [1]	Present
0·5	—	8·207	—	8·421
1	19·26	19·26	20·05	20·05

In the following section, the eigenvalues are used to identify the critical flutter load of the beam.

The flutter loads of cantilever Timoshenko beams are compared with the results obtained by using the classical theory, in Table 1. In general, the flutter loads based upon the Timoshenko theory are smaller than those based upon the classical one. The flutter loads of uniform beams obtained by the present method are in good agreement with the values obtained by other authors [1, 8].

2.2. ARTIFICIAL NEURAL NETWORKS

The multilayered perceptron network trained by means of the backpropagation algorithm is used here. A multilayered neural network is made of one or more hidden layers placed between the input layer and output layer. Each layer has a number of nodes connected with each of the nodes in the other layer. Thus the node in the lower layer is connected with every node in the higher layer. The information flow is only allowed in one direction during the training process, from the input layer to the output layer through the hidden layers. Each of the first hidden layer nodes obtains some information signals from the input layer nodes, and then the output of this layer gives some information signals into the second hidden layer nodes and so on.

Each node j in the layer $N-1$ is connected to each node i in the proceeding layer N through a connection of weight $W_{ij}^{N,N-1}$. The output signal passes through the neural network and the node j is expressed as [19]

$$x_i^N = f\left(\sum_{j=1}^{m} W_{ij}^{N,N-1}\, x_j^{N-1} - h_i^N \right), \tag{13}$$

where h_i^N is a threshold of the i-th neuron in the layer N. The $N = 1$ is the input layer and $N = F$ is the output layer.

The function $f(\,)$ is called the node activation function and assumed to be differentiable. For the hidden layers, the activation function is adopted to be a sigmoidal function

$$f(\beta) = \frac{1}{1 + \exp(-\beta)}, \quad \beta > 0. \tag{14}$$

For minimizing the errors seen at the output nodes, the backpropagation neural network algorithm is used here. The connection weights are developed during the training process. At the first step of training of the neural network, the connection weights are assigned random values. Once the input/output data for supervised learning are presented, the connection weights are modified in an iterative process during the training. At the successful completion of the training with minimum errors, the trained neural network is ready for use.

The backpropagation algorithm uses a gradient descent search method for minimizing an error defined as the mean-square difference between supervised output data d_i and actual output data x_i^F, i.e. the error J is given as

$$J = \sum_q \sum_i \frac{(d_i - x_i^F)}{2}, \tag{15}$$

where i is the number of output nodes, and q is the number of input/output patterns.

The error in the output layer on the backpropagation process is written as

$$\delta_i^F = -\frac{\mathrm{d}J}{\mathrm{d}\bar{x}_i^F} = (d_i - x_i^F) f_i'(\bar{x}_i^F) \tag{16}$$

and the error in any layer with the starting value of equation (16) is derived as

$$\delta_i^N = -\frac{\mathrm{d}J}{\mathrm{d}x_i^N} = f_i'(x_i^N) \sum_{j=1}^{m} (\delta_i^{N+1} W_{ij}^{N+1,N}), \tag{17}$$

$$x_i^N = \sum_{j=1} W_{ij}^{N,N-1} x_j^{N-1} \quad (N = F - 1, \ldots, 2, 1). \tag{18}$$

Then the new connection weights $\Delta W_{ij}^{N,N-1}$ is calculated by using equation (17):

$$\Delta W_{ij}^{N,N-1}(k+1) = \eta \delta_i^N x_{ij}^{N-1} + \alpha \Delta W_{ij}^{N,N-1}(k), \tag{19}$$

where η is termed a learning rate, which is chosen to be as large as possible (0·01 − 0·9) and α is a momentum term. The error δ_i^N must the calculated from the known error δ_i^F at the output layer. The errors are passed backwards through the network and a training algorithm uses the error to adjust the connection weights moving backwards from the output layer, layer by layer. The threshold is adjusted in the same way as the connection weights.

2.3. TRAINING AND TESTING OF NEURAL NETWORKS

The input data to train a neural network is very important. Kudva *et al.* [20] and Worden *et al.* [21] have presented the fault identification in a plate and framework structure using the neural network which was trained on the strain data. The

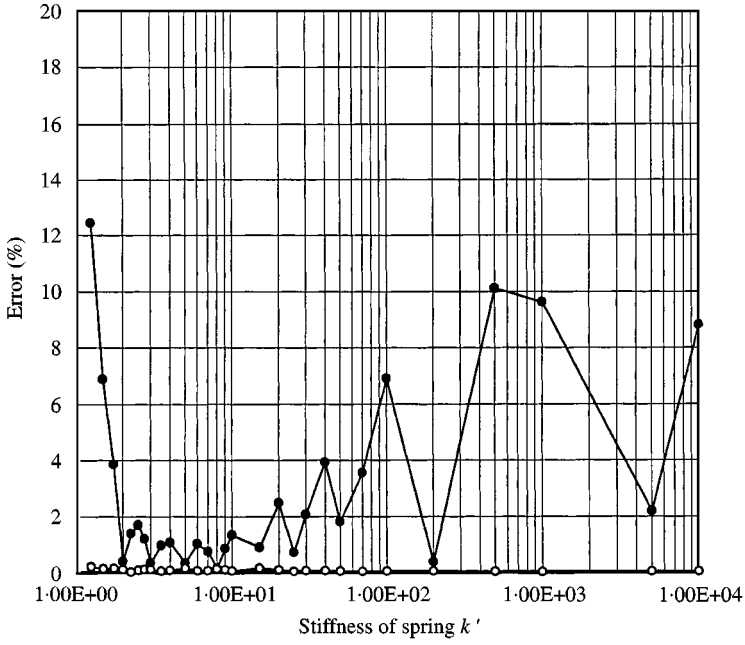

Figure 3. Error distribution of the stiffness and critical flutter load of the free-elastically restrained beam (learning pattern, $v = 0{\cdot}3$, $b_1/b_0 = 1{\cdot}0$, $h_1/h_0 = 0{\cdot}5$, $s_0 = 50$, $SSE = 0{\cdot}02$, ●: k', ○: p_{Bf}).

natural frequency is global and more stably measurable than the strain. Therefore, we use it as the input data.

The basic idea is to train a neural network with simulated patterns of the relative changes of natural frequencies and corresponding critical flutter load and boundary conditions of beams in order to recognize the behavior of the structure. Subjecting this neural network to un-learning natural frequencies should imply information about the critical flutter load and boundary conditions of beams.

The preparation of training data is a matter of considerable importance in artificial networks. If very little data is presented to the network, the training will give unsatisfactory results in that the internal features and relationships in the problem will not therefore be able to give reasonable approximations to un-learning test data. However, there are no generally accepted rules for determining the volume of training data and structure required. By a trial-and-error approach, with a view to simplify the network structure and speed up the convergence of the backpropagation algorithm, we defined the network of three layers with eight nodes in a hidden layer. The neural networks were trained with numerical values of the relative changes of the lowest four frequency parameters of beams.

In the first case, the neural networks were trained with numerical values of the relative changes in the lowest four frequency parameters ($\lambda_1 - \lambda_4$). The two output nodes were the stiffness of spring (k') and the critical flutter load of the elastically restrained-free beam (p_{Bf}). When subjecting the trained neural network to the training data sets, the error magnitudes on the stiffness of spring (k') and the corresponding critical flutter load (p_{Bf}) are shown in Figure 3. A final target

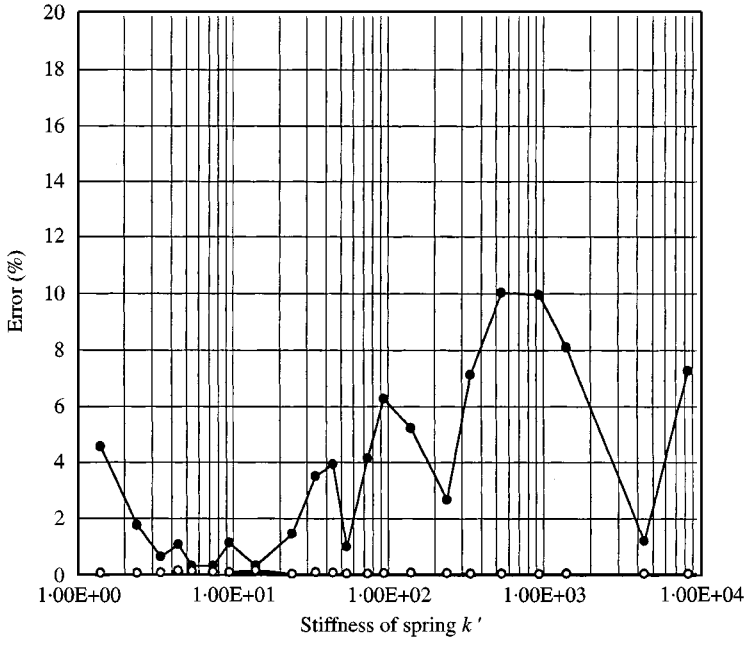

Figure 4. Error distribution of the stiffness and critical flutter load of the free-elastically restrained beam (un-learning pattern, $v = 0{\cdot}3$, $b_1/b_0 = 1{\cdot}0$, $h_1/h_0 = 0{\cdot}5$, $s_0 = 50$, $SSE = 0{\cdot}02$, ●: k', ○: p_{Bf}).

'summed squares error (SSE)', of the order of 0·02 average for the training pairs, is used for terminating the training process. The normalized input to the network was 29 training sets of data. The 22 sets of data were prepared for testing the trained networks. The error magnitude on the stiffness relatively increases after around the stiffness of 500, because the frequency parameter does not have the sensitivity to the stiffness in this range. On the other hand, the error magnitude on the critical flutter load is reduced by a factor of 10–50.

The important generalization capability of a network was tested by subjecting the trained network to testing data. The generalization capability is almost the same level as that of the trained network for the stiffness and flutter load, as shown in Figure 4. The capability for detecting the stiffness and critical flutter load with the error magnitude of 10% or less is sufficient in practice.

The error magnitudes on the slenderness ratio (s_0) and the corresponding critical flutter load (p_{Bf}) obtained by the trained network are shown in Figure 5. The two output nodes were the slenderness ratio and the critical flutter load of the cantilever beam. Although the large error occurs for the whole range of slenderness ratio, its magnitude rapidly improves and the number of epochs increases with decreasing SSE. The number of epochs has the same meaning as the CPU time. Both the error magnitude on the flutter load are much smaller than those on the slenderness ratio. The error magnitudes, when the trained network was subjected to nine testing sets of data, are shown in Figure 6. The generalization capability is almost comparable to that by the trained network, and its capability on SSE = 0·01 of estimating the slenderness ratio and flutter load is sufficient in practice with an error level of 10% or less except for under $s_0 = 20$.

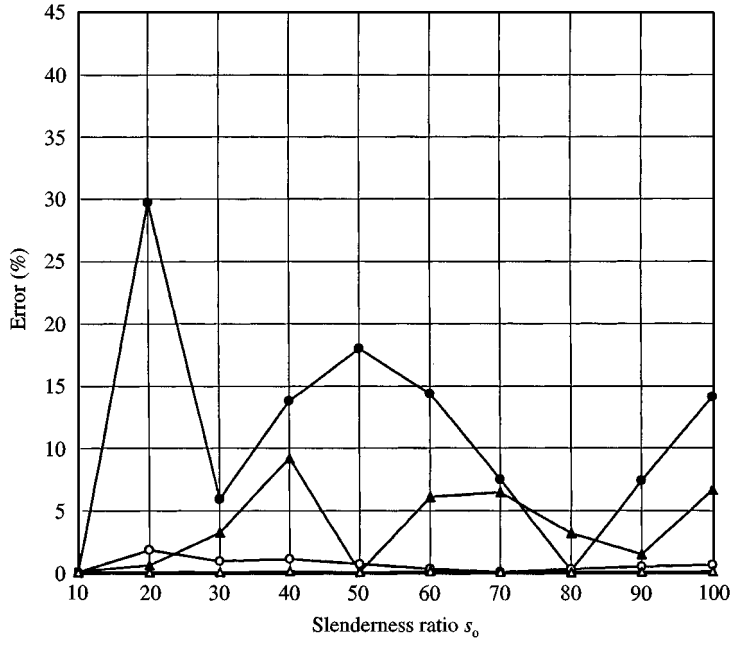

Figure 5. Error distribution of the slenderness ratio and critical flutter load of the cantilever beam (learning pattern, $v = 0{\cdot}3$, $b_1/b_0 = 1{\cdot}0$, $h_1/h_0 = 0{\cdot}5$, *SSE*: (●, s_0, ○, p_{Bf}), 0·05; (▲, s_0; △, p_{Bf}), 0·01).

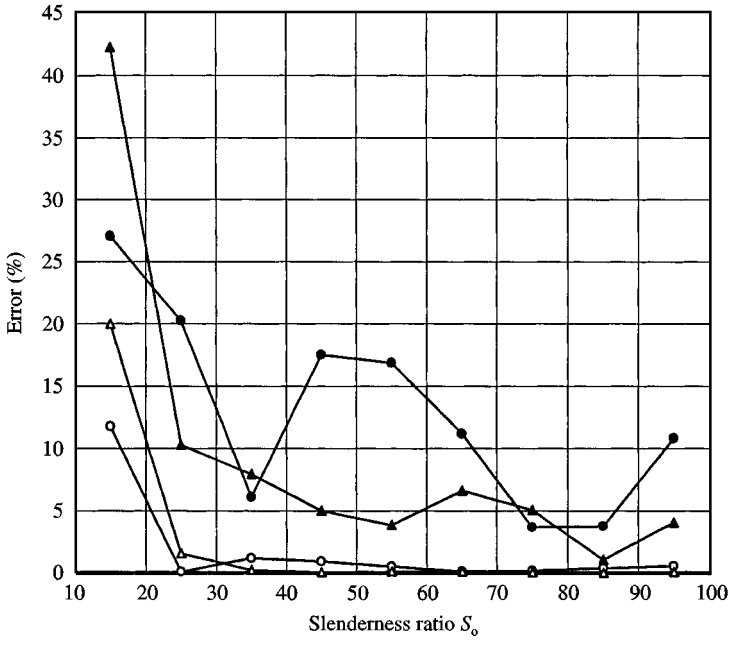

Figure 6. Error distribution of the critical flutter load of the cantilever beam (un-learning pattern, $v = 0{\cdot}3$, $b_1/b_0 = 1{\cdot}0$, $h_1/h_0 = 0{\cdot}5$, *SSE*: (●, s_0, ○, p_{Bf}), 0·05; (▲, s_0; △, p_{Bf}), 0·01).

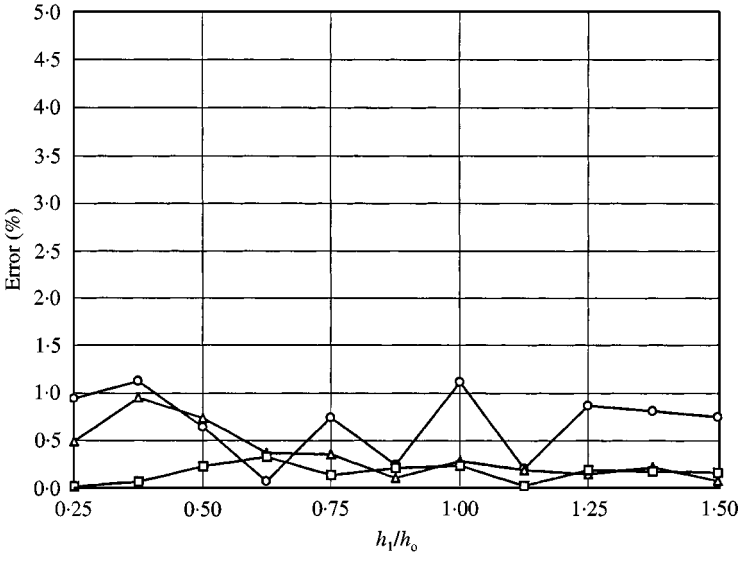

Figure 7. Error distribution of the taper ratio of the cantilever beam (learning pattern, $v = 0{\cdot}3$, $b_1/b_0 = 1{\cdot}0$, $s_0 = 50$, *SSE*: ○, 0·0005; △, 0·0001; □, 0·00005).

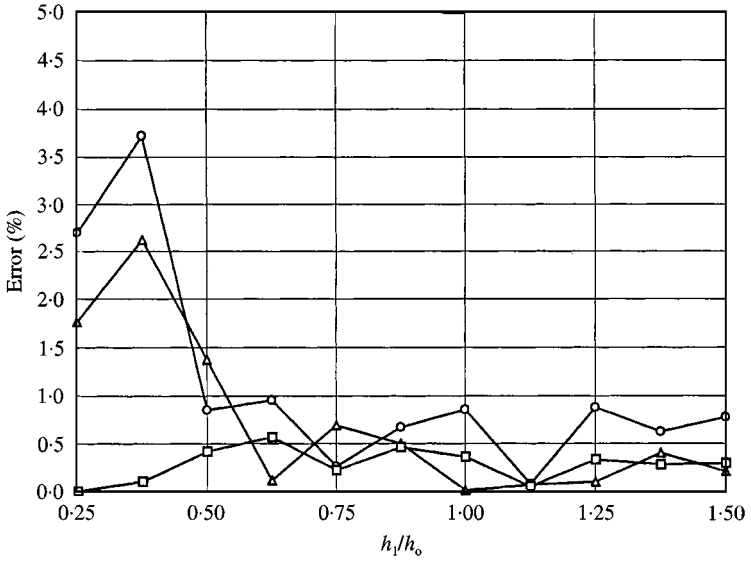

Figure 8. Error distribution of the critical flutter load of the cantilever beam (learning pattern, $v = 0{\cdot}3$, $b_1/b_0 = 1{\cdot}0$, $s_0 = 50$, *SSE*: ○, 0·0005; △, 0·0001; □, 0·00005).

Figures 7 and 8 show the error magnitudes on the taper ratio (h_1/h_0) and the corresponding critical flutter load (p_{Bf}) obtained by the trained networks respectively. The two output nodes were the taper ratio and the critical flutter load of the cantilever beam. Both error magnitudes are much smaller than those in the previous two cases. The error magnitude for the taper ratio is reduced by a factor of

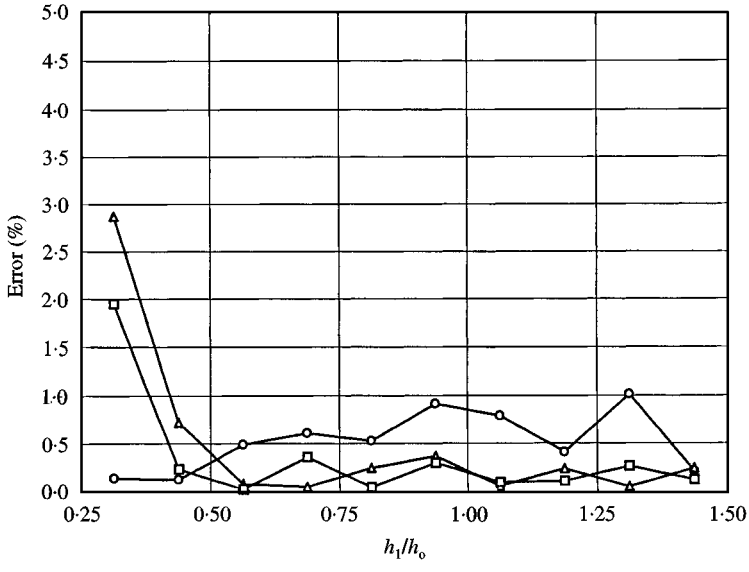

Figure 9. Error distribution of the taper ratio of the cantilever beam (un-learning pattern, $v = 0{\cdot}3$, $b_1/b_0 = 1{\cdot}0$, $s_0 = 50$, *SSE*: ○, 0·0005; △, 0·0001; □, 0·00005).

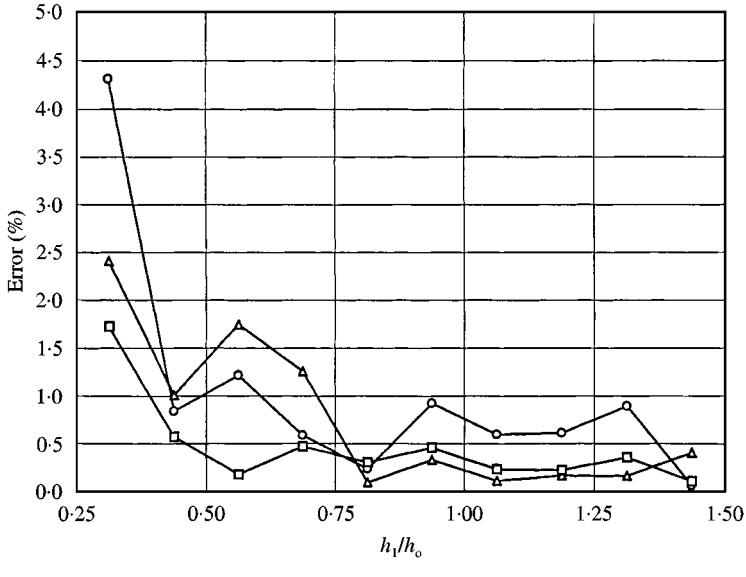

Figure 10. Error distribution of the critical flutter load of the cantilever beam (un-learning pattern, $v = 0{\cdot}3$, $b_1/b_0 = 1{\cdot}0$, $s_0 = 50$, *SSE*: ○, 0·0005; △, 0·0001; □, 0·00005).

10, compared with that for slenderness ratio or stiffness. The error magnitudes are not so radically affected by the SSE in smaller range and the "over-learning phenomenon" did not occur in this range. When subjecting the trained network to 10 testing sets of data, the error magnitudes on the taper ratio and the flutter load are shown in Figures 9 and 10 respectively. The generalization capabilities for both parameters are also excellent.

3. CONCLUSIONS

In this paper a Multilayer Perceptron network trained with the Backpropagation Algorithm was applied for detecting the critical flutter load and boundary conditions (or other shape parameters) in the structural element. Numerical examples were presented to demonstrate the possibility of the network. From the results of the numerical examples we can draw the following conclusions. First, the critical flutter load and boundary conditions can be predicted by the change in frequency parameters. Second, the one hidden layer of trained network is sufficient to identify them.

ACKNOWLEDGMENT

The author would like to thank M. Yamamoto, a student of *Kanagawa Institute of Technology*, for the calculations in the study.

REFERENCES

1. V. V. Bolotin 1963 *Nonconservative Problems of Theory of Elastic Stability*. Oxford: Pergamon Press.
2. H. Leipholz 1980 *Stability of Elastic Systems*. The Netherlands: Sijthoff & Noordhoff.
3. H. Saito and K. Otomi 1979 *Journal of Sound and Vibration* **62**, 257. Vibration and stability of elastically supported beams carrying an attached mass under axial and tangential loads.
4. T. Irie, G. Yamada and I. Takahashi 1980 *Journal of Sound and Vibration* **70**, 503. Vibration and stability of a non-uniform Timoshenko beam subjected to a follower force.
5. S. Y. Lee, Y. H. Kuo and F. Y. Lin 1992 *Journal of Sound and Vibration* **153**, 193. Stability of a Timoshenko beam resting on a Winkler elastic foundation.
6. S. Y. Lee and C. C. Yang 1994 *Journal of Sound and Vibration* **169**, 433. Non-conservative instability of non-uniform beams resting on an elastic foundation.
7. M. A. De Rosa and C. Franciosi 1990 *Journal of Sound and Vibration* **137**, 107. The influence of an intermediate support on the stability behavior of cantilever beams subjected to follower forces.
8. I. Takahashi and T. Yoshioka 1996 *Computers and Structures* **59**, 1033. Vibration and stability of a non-uniform double-beam subjected to follower forces.
9. T. Master 1995 *Neural, Novel and Hybrid Algorithms for Time Series Prediction*. New York, Wiley.
10. S. Haykin 1994 *Neural Networks*. New York: Macmillan Publishing Company, Inc.
11. M. H. Hassoun 1995 *Artificial Neural Networks*. Cambridge, MA: The MIT Press.
12. I. Takahashi and T. Yoshioka 1995 *Proceedings of CIVIL-COMP 1995*, *Developments in Neural Networks and Evolutionary Computing for Civil and Structural Engineering*, 15. Use of neural networks for fault identification in a beam structure.
13. K. Yasuda and Y. Goto 1994 *Bulletin of JSME* **570**, 118. Experimental identification technique for boundary conditions of a beam.
14. K. Kamiya, K. Yasuda and H. Miya 1995 Bulletin of JSME **587**, 212. Experimental identification of a nonlinear beam.
15. H. Sato, Y. Iwata and S. Sugimoto 1995 *Bulletin of JSME* **585**, 152. Identification of non-linear support systems by using transient respose.
16. I. Takahashi 1997 *Proceedings of the* 1997 *International Conference on Engineering Applications of Neural Networks*, *Neural Networks in Engineering Systems*, 253, Identification for axial force and boundary conditions of a beam using neural networks.

17. G. R. Cowper 1966 *Journal of Applied Mechanics* **33**, 335. The shear coefficients in Timoshenko's beam theory.
18. A. N. Kounadis and J. T. Katsikadelis 1976 *Journal of Sound and Vibration* **49**, 171. Shear and rotatory inertia effects on Beck's column
19. M. Yagawa 1992 *Neural Network*. Tokyo: Baihuukan Press (in Japanese).
20. J. Kudva, N. Munir and P. W. Tan 1992 *Smart Material and Structure* **1**, 108. Damage detection in amart structures using neural networks and finite-element analysis.
21. K. Worden, A. D. Ball and G. R. Tomlinson 1993 *Proceedings of* 11*th International Modal Analysis Conference*, Vol. 1, 47. Fault location in structures using neural networks.